# Numerical Analysis of Control of Flow Oscillations in Open Cavity Using Moving Bottom Wall*

Takashi YOSHIDA**, Takashi WATANABE***, Toshihiko IKEDA** and Shouichiro IIO**

In this study, we investigate the active control of self-sustained oscillating flow over an open cavity using a moving bottom wall. The incompressible Navier-Stokes equations are solved using finite difference methods for the two-dimensional cavity with laminar boundary layer upstream. We move the cavity bottom wall tangentially with nondimensional velocities ranging from −0.2 to +0.2. The results show that wall velocity changes the characteristics of recirculating flow in the cavity and that the modification of recirculating flow plays an important role in changing the oscillation characteristics of the separated shear layer. When the wall velocity is less than −0.1, two recirculating vortices change to one clockwise recirculating vortex in the cavity, so that the self-excited shear layer oscillations are completely suppressed. When the wall velocity is more than +0.19, two stationary vortices exist on the upper side and lower side of the cavity and the self-excited shear layer oscillations are suppressed.

***Key Words***: Computational Fluid Dynamics, Finite Difference Method, Cavity Flow, Incompressible Flow, Oscillatory Flow, Self-Sustained Oscillation, Flow Control

## 1. Introduction

Flows over cavities occur in a wide variety of engineering applications, for example, the wheel wells of aircrafts, sunroofs and windows of automobiles, and spaces between bullet train cars. Cavity flow was the focus of much attention of many investigators in the past because of its fundamental interest. Despite its geometrical simplicity, the flow over a cavity is characterized by a complex feedback mechanism that leads to self-sustained oscillations of a separated shear layer. The feedback process consists of the following loop of events: shear layer instability and the growth of vortices, the impingement of the vortices at the downstream edge, the generation of hydrodynamic or acoustic pressure disturbances, the upstream propagation of these disturbances, influence on the receptive region of the shear layer near the upstream leading edge of the cavity, the conversion of this influence into new vertical fluctuations, and the amplification of the vortical perturbations with convection by the shear layer resulting in a new impingement. However, there still remain many questions about even the basic physical mechanisms underlying the self-sustained oscillations. Flow-induced cavity oscillations have been classified by Rockwell and Naudascher[1] into fluid-dynamic and fluid-resonant. Incompressible flows such as low-Mach number air flows, low-speed water flows over a cavity are classified as fluid-dynamic oscillations. For this condition, the acoustic wavelength is much longer than the length of the cavity and the feedback mechanism can be regarded as purely hydrodynamic. In this investigation, we assume that the flow has a very low-Mach number or is a low-speed liquid flow and we regard the fluid as incompressible.

The suppression of cavity flow oscillations has received considerable attention in recent years. The control of cavity oscillations has been reviewed by Cattafesta et al.[2] Numerous workers have used various control devices, for example, piezoelectric flaps, pulsed blowing actuators, fixed fences, spoilers, and ramps. They reported the suppression of oscillations by the control of a separated shear layer using these devices.

Kuo and Huang[3] studied the effect of a sloped bottom of a shallow cavity (cavity length to depth ratio, $L/D = 2$). They noted the role of large-scale vortex struc-

* Received 6th February, 2006 (No. 06-4047)

** Department of Environmental Science and Technology, Shinshu University, 4–17–1 Wakasato, Nagano-shi, Nagano 380–8553, Japan.
E-mail: yoshi-t@shinshu-u.ac.jp

*** EcoTopia Science Institute, Nagoya University, Furo-cho Chikusa-ku, Nagoya-shi, Aichi 464–8603, Japan

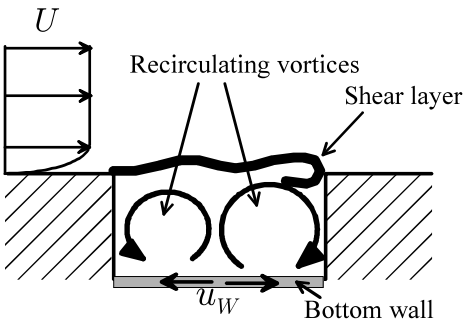


Fig. 1 Sketch of cavity flow with moving bottom wall

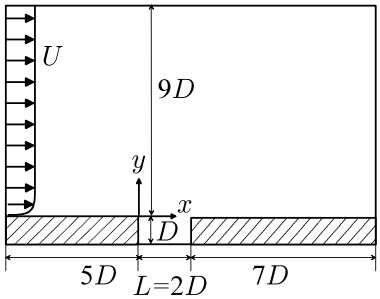


Fig. 2 Schematic diagram of cavity configuration and computational domain

tures in the cavity and their interaction with shear layers. They reported that a sloped bottom of the cavity changes recirculation vortices and the modified recirculation flow perturbs the unstable shear layer. Shear layer oscillations are completely suppressed in the case of a large sloped bottom. Their results show that the recirculation flow inside the cavity also plays an important role in the sustainment of shear layer oscillations. Pereira and Sousa[4] investigated the unsteady characteristics of self-sustained shear layer oscillations for an $L/D = 2$ cavity by the two-dimensional numerical simulation of incompressible Navier-Stokes equations. They also noted that the shear layer instability process involves a complex coupling of the shear layer and recirculating flow field dynamics. These results suggest that it is possible to control shear layer oscillations by a modification of the recirculating flow field within the cavity.

In this study, we focused on the role of recirculation vortices in the cavity in shear layer oscillations and on the simple active control of the recirculating flow and cavity oscillations. The interaction between recirculating flow field and shear layer oscillations has been neglected in most previous studies. The basic idea of our control method is to drive the bottom wall with a constant velocity tangentially to itself, which is similar to the lid-driven cavity flow problem. The bottom wall of the cavity moves horizontally with either a positive or a negative constant velocity, $u_W$, as shown in Fig. 1. The moving bottom wall can produce shear stress in fluid and change recirculating vortices in the cavity. This control method is classified into active control according to the classification by Cattafesta et al.[2] In this study, we examine the following issues: what are the effects of the moving wall on cavity flow dynamics and how effective is this control method in attenuating shear layer oscillations? We perform two-dimensional Navier-Stokes simulations for the incompressible flow with and without a moving bottom wall and present the suppressive effect of a moving bottom wall on cavity oscillations.

## 2. Numerical Methods

The governing equations are the incompressible two-dimensional Navier-Stokes equations and the equation of continuity,

$$\frac{\partial u}{\partial t}+u\frac{\partial u}{\partial x}+v\frac{\partial u}{\partial y}=-\frac{\partial p}{\partial x}+\frac{1}{Re}\left(\frac{\partial^2 u}{\partial x^2}+\frac{\partial^2 u}{\partial y^2}\right), \tag{1}$$

$$\frac{\partial v}{\partial t}+u\frac{\partial v}{\partial x}+v\frac{\partial v}{\partial y}=-\frac{\partial p}{\partial y}+\frac{1}{Re}\left(\frac{\partial^2 v}{\partial x^2}+\frac{\partial^2 v}{\partial y^2}\right), \tag{2}$$

$$\frac{\partial u}{\partial x}+\frac{\partial v}{\partial y}=0, \tag{3}$$

where all variables are nondimensionalized using the cavity depth $D$ and the free-stream velocity $U$. These equations were integrated in time using the semi-implicit splitting method by Dukowicz and Dvinsky[5] to enforce the solenoidal condition, in which the backward Euler method was used for the viscous terms and the forward Euler method was used for the other terms. A nonuniform staggered grid system, which clusters node points in the boundary layer, shear layer, the cavity bottom, and cavity edges, was used for spatial descretization. The third order upwind-biased difference scheme was used for the convective terms and the second order central difference scheme was used for the other terms. The finite difference formula for the nonuniform spaced grids were derived using Fornberg's algorithm[6].

A schematic diagram of the cavity configuration and computational domain are shown in Fig. 2. The cavity length to depth ratio is $L/D = 2$, which is the same as that used in the condition of Kuo and Huang's experiment[3]. The computational domain extends to $5D$ upstream of the cavity leading edge, $7D$ downstream of the trailing edge and $9D$ in the normal direction above the cavity. This dimension of the computational domain is similar to that used in the two-dimensional simulations of Rowley et al.[7] The laminar Blasius boundary layer is specified in the inflow boundary. $U$ is the free-stream velocity outside the laminar boundary layer. The bottom-wall velocity $u_W$ shown in Fig. 1 is nondimensionalized by $U$. Time $t$ is nondimensionalized by $D/U$. The time $t^*$ is the nondimensional time elapsed after the sudden start of the movement of the bottom wall. A free-slip condition was applied to the normal boundary. A no-slip boundary condition was applied to the wall. At the outflow boundary, we used the

Sommerfeld radiation condition, which is also called the convective outflow condition. This condition is written as

$$\frac{\partial \phi}{\partial t} + U_C \frac{\partial \phi}{\partial x} = 0, \tag{4}$$

where $\phi$ is any velocity component. The convective velocity $U_C$ is set equal to the mean velocity integrated across the exit boundary. This boundary condition allows vortices to smoothly pass across the computational domain.

## 3. Results

### 3.1 Baseline flow

The baseline flow is a flow over a cavity with a stationary bottom wall. The Reynolds number based on $U$ and $D$, $Re = UD/\nu$, was 6 000. The oncoming laminar boundary layer had a thickness $\delta$ of 0.235, a displacement thickness $\delta^*$ of 0.081 and a momentum thickness $\theta$ of 0.031 at the upstream edge of the cavity. The Reynolds number based on $\theta$, $Re_\theta = U\theta/\nu$, was 186. These Reynolds numbers are similar to those used in Kuo and Huang's study using a water channel.

The computational results were validated by performing mesh refinement studies to ensure that the results are independent of mesh dimension. Three meshes were examined: 175×80 and 75×25, 350×160 and 150×50, and 525×240 and 225×75 points in the computational domain in the streamwise and streamwise-normal directions and in the cavity, respectively. Figure 3 shows the spectra of the normal velocity $v$ at $x = 1.9$ and $y = 0$ for the three different meshes. The most dominant peak and other harmonic peaks in the spectrum of the medium mesh (350×160) was similar to those of the fine mesh (525×240). Figure 4 shows the stream lines for the three different meshes at the same phase of self-sustained oscillations. The flow pattern of the medium mesh (350×160) was similar to those of the fine mesh (525×240). We concluded that the medium mesh (350×160) is adequate for resolving the flow and was used in this study. The time step was $\Delta t = 0.001$, and the corresponding maximum Courant number was about 0.18.

The unsteady characteristics of fluid-dynamic oscillations are clearly supported by the computational results. The time traces of normal velocity and pressure at $x = 1.9$ and $y = 0$ near the downstream edge of the cavity are shown in Fig. 5. The fluctuations of normal velocity and pressure are alomost periodic. The corresponding power spectra of normal velocity and pressure are

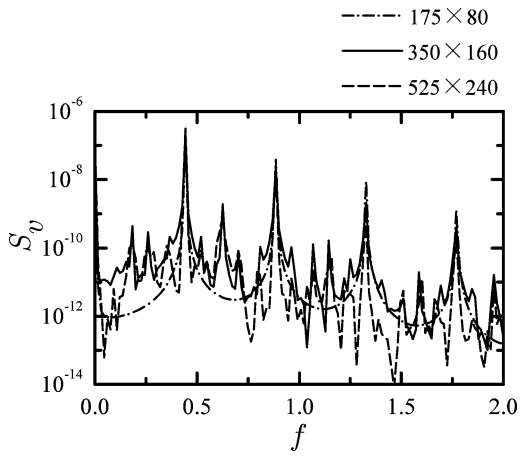


Fig. 3 Comparison of mesh refinement power spectra of normal velocity at $x = 1.9$ and $y = 0$

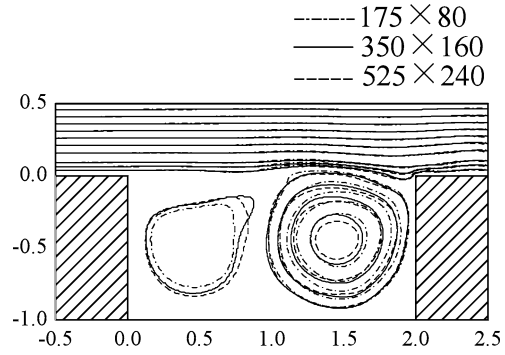


Fig. 4 Comparison of mesh refinement stream lines at the same phase of self-sustained oscillations

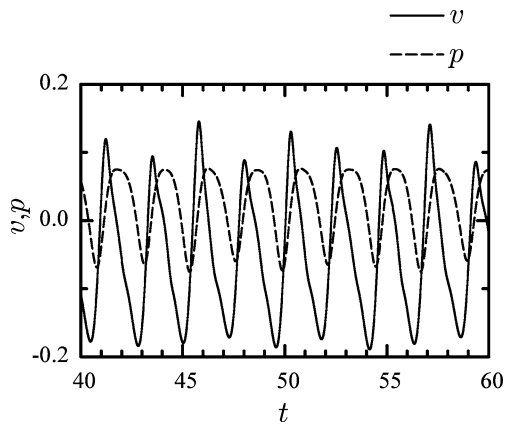


Fig. 5 Time traces of normal velocity and pressure at $x = 1.9$ and $y = 0$ for baseline case

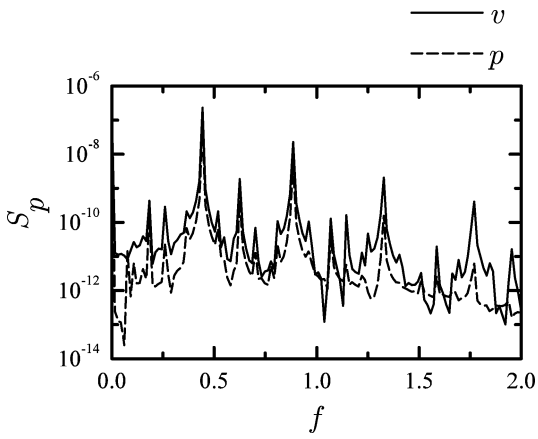


Fig. 6 Power spectra of normal velocity and pressure at $x = 1.9$ and $y = 0$ for baseline case

shown in Fig. 6. The very well-defined dominant peaks and higher harmonics of both spectra are evident. The frequencies of the most energetic peaks of both spectra are identical and the Strouhal number based on the cavity depth is $St = 0.443$.

The Strouhal number based on the momentum thickness at the upstream edge of the cavity was $St_\theta = 0.013\,7$. In Fig. 7, the Strouhal number obtained in the present computation is compared with the previous experimental data obtained by Knisely and Rockwell[8] and Kuo and Huang[3]. Our result closely agrees with the solid curve fitted to the measured data of Knisely and Rockwell. Our present result for an $L/D = 2$ cavity shows that self-sustained oscillations in the cavity shear layer are in mode II. There are two wavelengths in the cavity in mode II as observed by Gharib and Roshko[9].

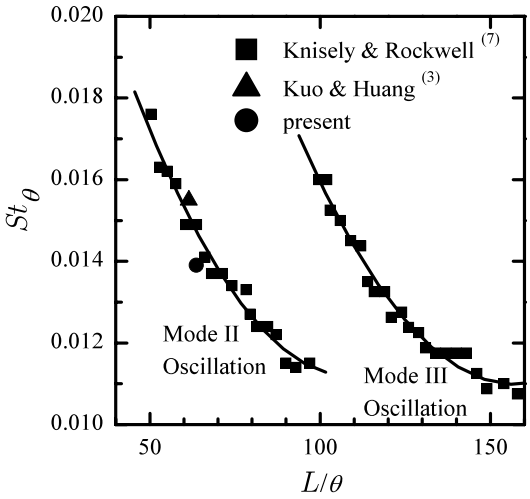


Fig. 7 Comparison of Strouhal number based on momentum thickness at upstream edge of cavity for baseline case with experimental data

Figure 8 shows four images of vorticity gray scale contour plots and streamlines over one period of oscillation. The cavity is occupied by two stationary vortices. One is a strong clockwise rotating vortex on the downstream side of the cavity and the other is a weak counterclockwise rotating vortex on the upstream side. The small clockwise vortex develops in the separation region due to the Kelvin-Helmholtz instability (see Fig. 8 (d) and (a)). The third vortex travels over the counterclockwise vortex (see Fig. 8 (b) and (c)) and pairs with the clockwise rotating vortex on the downstream side (see Fig. 8 (d) and (a)). The shear layer vortex travels over the downstream side vortex and impinges on the corner.

### 3.2 Effect of moving bottom wall with negative velocity

A series of computations for the moving bottom wall with a negative velocity, $u_W < 0$, was conducted over a range of $u_W$ from $-0.02$ to $-0.2$. The initial condition was the instantaneous flow field of the baseline flow and the

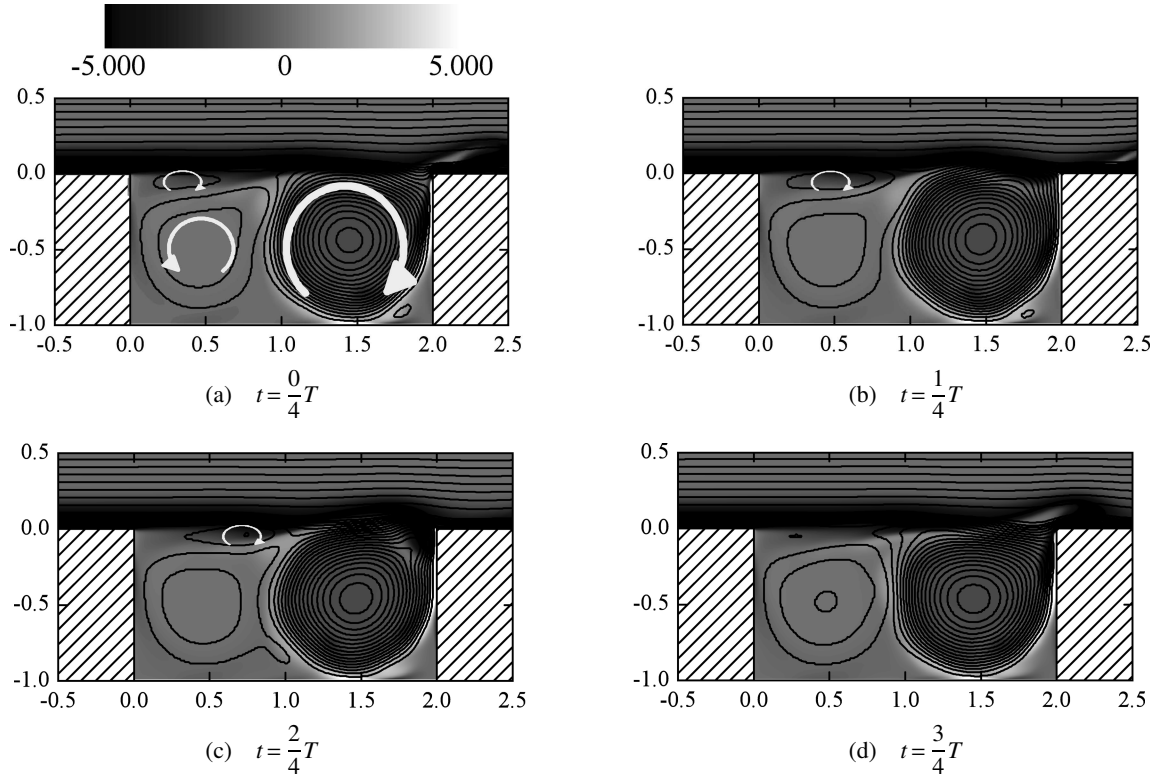


Fig. 8 Instantaneous streamlines (solid lines) and gray scale contour plots of vorticity for $u_W = 0$ at four different times, corresponding to quarter-phase intervals of periodic cycle, $T$

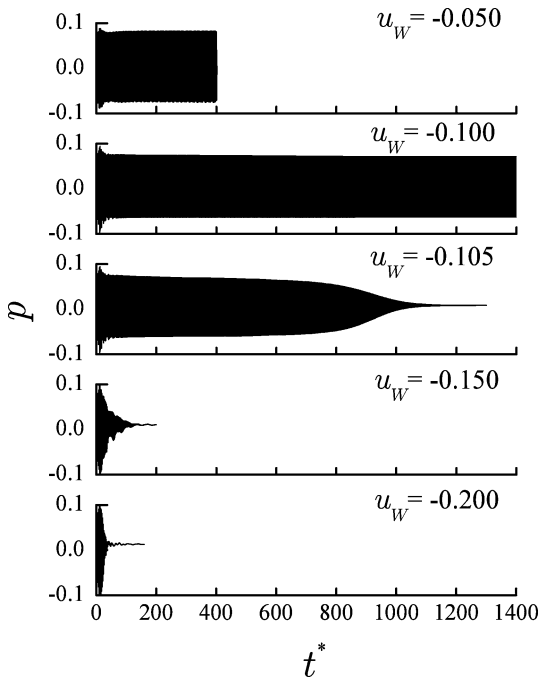


Fig. 9 Time traces of pressure at $x = 1.9$ and $y = 0$ for different negative velocities of bottom wall

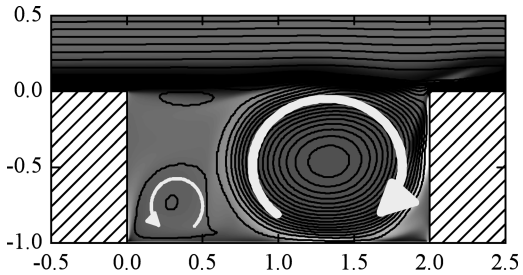

Fig. 10 Instantaneous streamlines (solid lines) and gray scale contour plot of vorticity at $t^* = 1\,400$ for $u_W = -0.100$

bottom wall was suddenly started at $t^* = 0$. The typical time traces of pressure at $x = 1.9$ and $y = 0$ are shown in Fig. 9 for runs where $u_W$ was varied. These calculations were stopped at different time points. For $u_W > -0.1$, the oscillations are maintained. For $u_W = -0.105$, the oscillations are slowly damped and the flow becomes steady. As for increasing negative wall velocity, the oscillations are reduced more rapidly and are suppressed completely.

Figure 10 shows streamlines and a vorticity contour plot at $t^* = 1\,400$ for $u_W = -0.100$. In the cavity, the clockwise vortex on the downstream side becomes larger and the counterclockwise vortex on the upstream side disappears because of negative wall shear stress. A new small clockwise vortex develops near the upstream corner. The separated shear layer becomes unstable and maintains oscillations. In Fig. 11, flow fields at two different times are given for $u_W = -0.105$. In Fig. 11 (a), the flow field is similar to that for $u_W = -0.100$ during oscillations. The upstream small vortex disappears while the oscillations are

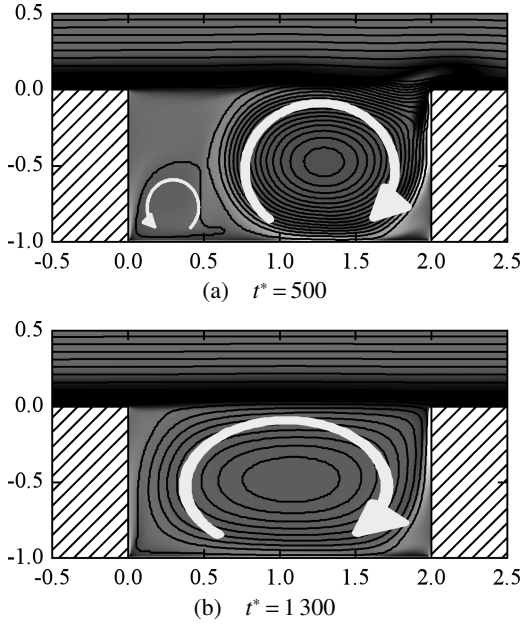


Fig. 11 Instantaneous streamlines (solid lines) and gray scale contour plots of vorticity for $u_W = -0.105$

damping, and the downstream clockwise vortex occupies the entire space inside the cavity as shown in Fig. 11 (b). The flow on the upper side of the cavity is parallel to the separated shear layer over the entire cavity mouth, so that the shear layer becomes stable and the oscillations are suppressed.

### 3.3 Effect of moving bottom wall with positive velocity

The response of the flow over the cavity to a positive bottom wall velocity differs from that to a negative wall velocity. The wall velocity $u_W$ was changed from +0.02 to +0.2. Figure 12 shows the typical time traces of pressure at $x = 1.9$ and $y = 0$. These calculations were stopped at different time points. For $u_W = +0.050$, the oscillations are preserved and there is little change in the amplitude of pressure fluctuation. For $+0.190 \geq u_W \geq +0.070$, the oscillating amplitude of pressure damps rapidly and the shear layer oscillations are suppressed, but after a long interval, the self-sustained oscillations restart. For $u_W \geq +0.195$, the oscillations are almost suppressed.

The changes in the flow patterns for a positive wall velocity are shown in following figures. Figure 13 shows streamlines and a vorticity contour plot at $t^* = 500$ for $u_W = +0.050$. The configuration of two vortices in the cavity is similar to that for $u_W = 0$, although the clockwise vortex on the downstream side becomes smaller and the counterclockwise vortex on the upstream side becomes larger than those shown in Fig. 8. As the wall speed increases up to +0.190, the shear layer oscillations are initially suppressed and recur after a long time. Figure 14 shows the instantaneous streamlines and vorticity fields for $u_W = +0.190$. The third clockwise vortex develops near

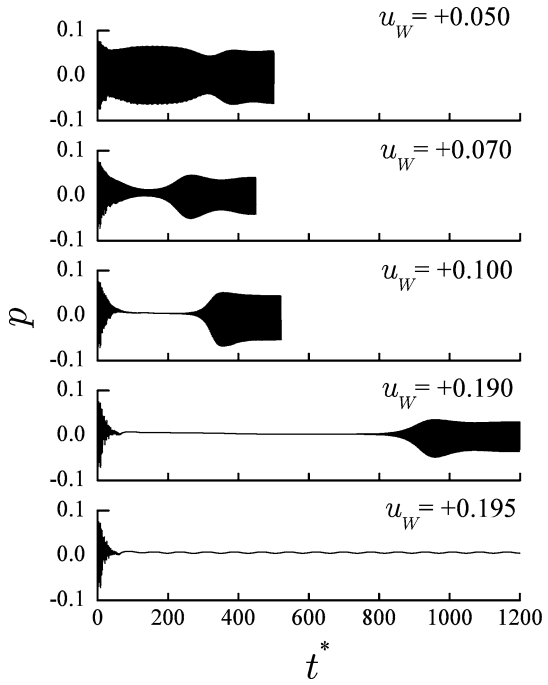


Fig. 12 Time traces of pressure at $x = 1.9$ and $y = 0$ for different positive velocities of bottom wall

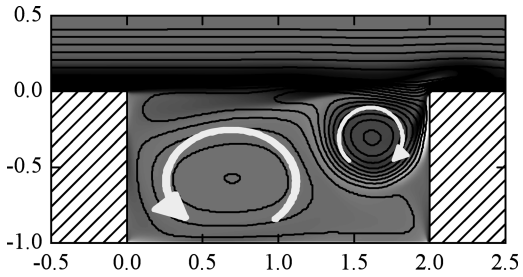

Fig. 13 Instantaneous streamlines (solid lines) and gray scale contour plot of vorticity at $t^* = 500$ for $u_W = +0.050$

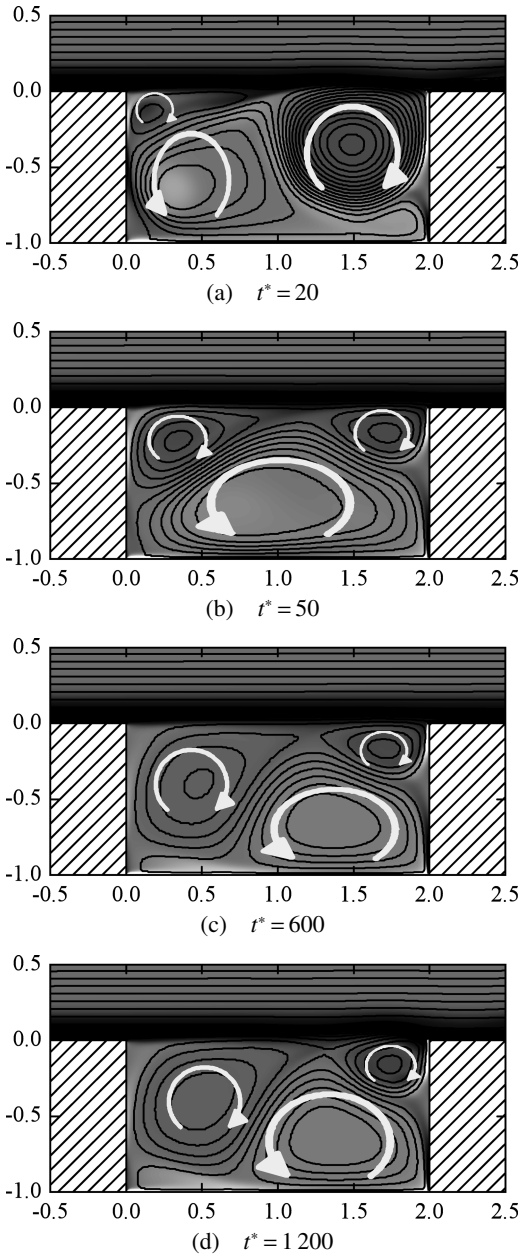


Fig. 14 Instantaneous streamlines (solid lines) and gray scale contour plots of vorticity for $u_W = +0.190$

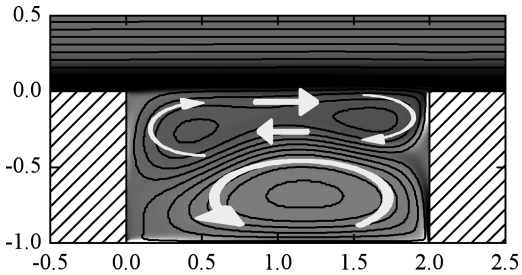

Fig. 15 Instantaneous streamlines (solid lines) and gray scale contour plot of vorticity at $t^* = 1\,200$ for $u_W = +0.195$

the upstream edge of the cavity as shown in Fig. 14 (a) and (b) and the flow oscillations are suppressed. The clockwise rotating vortex on the downstream side of the cavity becomes small and moves near the downstream edge of the cavity and the counterclockwise vortex moves under the clockwise rotating vortex during the shear layer oscillations are suppressed as shown in Fig. 14 (c). Then three vortices exist inside the cavity and the flow oscillations recur as shown in Fig. 14 (d). Figure 15 shows a steady flow field for $u_W = +0.195$ when the oscillations are suppressed. The two clockwise vortices merge into one vortex, which occupies the upper region inside the cavity. Figure 15 shows a phenomenon in which one dominant clockwise vortex covers a full region of the cavity mouth. The dominant vortex can be found in the flow in Fig. 11 (b), and this vortex suppresses the flow oscillations, as has been said in section 3.2.

## 4. Conclusions

A numerical study of the active control of self-sustained oscillating flow over an open cavity using a moving bottom wall was conducted. Our control method involves the moving of the bottom wall tangentially with a constant velocity $u_W$. The two-dimensional incompressible Navier-Stokes equations were solved using finite difference methods for the uncontrolled case and controlled cases. The results for the uncontrolled case reasonably demonstrate the characteristics of self-sustained shear layer oscillations. The effect of the moving bottom wall is shown by the results for the controlled cases. For the negative wall speed, a single clockwise vortex occupies the cavity and the shear layer oscillations are suppressed for $u_W \leq -0.105$. For the positive wall speed, two vortices, which lie horizontally, occupies the cavity and the shear layer oscillations are suppressed for $u_W \geq +0.195$.

## References


( 1 ) Rockwell, D. and Naudascher, E., Review—Self-Sustaining Oscillations of Flow Past Cavities, Trans. ASME, J. Fluids Eng., Vol.100 (1978), pp.152–165.

( 2 ) Cattafesta, L., Williams, D., Rowley, C. and Alvi, F., Review of Active Control of Flow-Induced Cavity Resonance, AIAA 2003-3567, (2003), pp.1–20.

( 3 ) Kuo, C.H. and Huang, S.H., Influence of Flow Path Modification on Oscillation of Cavity Shear Layer, Experiments in Fluids, Vol.31 (2001), pp.162–178.

( 4 ) Pereira, J.C.F. and Sousa, J.M.M., Experimental and Numerical Investigation of Flow Oscillations in a Rectangular Cavity, Trans. ASME, J. Fluids Eng., Vol.117 (1995), pp.68–74.

( 5 ) Dukowicz, J.K. and Dvinsky, A.S., Approximate Factorization as a High Order Splitting for the Implicit Incompressible Flow Equations, J. Comput. Phys., Vol.102 (1992), pp.336–347.

( 6 ) Fornberg, B., Generation of Finite Difference Formulas on Arbitraily Spaced Grids, Mathematics of Computation, Math. Comput., Vol.51, No.184 (1988), pp.699–706.

( 7 ) Rowley, C.W., Colonius, T. and Basu, A.J., On Self-Sustained Oscillations in Two-Dimensional Compressible Flow over Rectangular Cavities, J. Fluid Mech., Vol.455 (2002), pp.315–346.

( 8 ) Knisely, C. and Rockwell, D, Self-Sustained Low-Frequency Components in an Impinging Shear Layer, J. Fluid Mech., Vol.116 (1982), pp.157–186.

( 9 ) Gharib, M. and Roshko, A, The Effect of Flow Oscillations on Cavity Drag, J. Fluid Mech., Vol.177 (1987), pp.501–530.